

## Dynamic analysis of a small-sized wind turbine in the Midwest of Brazil

<http://dx.doi.org/10.1590/0370-44672023770048>

**Yago Machado Pereira de Matos**<sup>1,3</sup>

<https://orcid.org/0000-0003-4676-5140>

**Márcio Muniz de Farias**<sup>1,4</sup>

<https://orcid.org/0000-0002-5257-911X>

**Renato Pinto da Cunha**<sup>1,5</sup>

<https://orcid.org/0000-0002-2264-9711>

**Marlos José Ribeiro Guimarães**<sup>2,6</sup>

<https://orcid.org/0009-0000-7860-0020>

**Renato Marques Cabral**<sup>2,7</sup>

<https://orcid.org/0000-0002-4723-8521>

<sup>1</sup>Universidade de Brasília - UnB,  
Departamento de Engenharia Civil e Ambiental,  
Brasília - Distrito Federal - Brasil.

<sup>2</sup>Eletrobras Furnas,  
Departamento de Segurança de Barragens e Tecnologia,  
Aparecida de Goiânia - Goiás - Brasil.

E-mails : <sup>3</sup>[yago\\_mpm@hotmail.com](mailto:yago_mpm@hotmail.com), <sup>4</sup>[muniz@unb.br](mailto:muniz@unb.br),  
<sup>5</sup>[rpcunha@unb.br](mailto:rpcunha@unb.br), <sup>6</sup>[marlos@furnas.com.br](mailto:marlos@furnas.com.br),  
<sup>7</sup>[renatocg@furnas.com.br](mailto:renatocg@furnas.com.br)

### Abstract

Nowadays, despite the implementation of new wind farms in Brazil, it still is difficult to form partnerships with companies in the sector, which significantly contributes to the gap in information provided by national literature and the lack of knowledge about the mechanical behavior of wind turbines subjected to transient wind effects. Therefore, through a Research and Development Project to optimize and improve modeling in wind systems, the Brazilian electric power company Eletrobras Furnas aims to facilitate the construction of smaller wind turbines to supply energy to regions far from the Brazilian coast that do not have high generation potential due to the incidence of low-speed winds. Two relevant aspects directly linked to the performance of this kind of structures are: (i) determining their natural frequency and (ii) ensuring that this frequency does not coincide with any external vibration frequency that the structure may experience in its lifetime. Wind turbines are complex systems with many degrees of freedom and their own frequencies associated with the respective mode shapes in which they naturally vibrate. These frequencies are inversely related to the mass and directly related to the stiffness of the structure. Thus, through numerical modeling using the Finite Element Method, the present article aims to list some of the main factors that can affect the prediction of the natural frequency of a real-scale wind turbine prototype and to evaluate its dynamic behavior, considering its rotor revolution frequency, its blade passing frequency and the wind characteristics of its operating area.

**Keywords:** small-sized wind turbine, finite element method, natural frequencies, dynamic analysis.

### 1. Introduction

As the world's population density increases, access to energy has increasingly become a very important issue in modern society. There are many ways of producing energy, and each method has their own benefits and disadvantages. Ideally, the selected method should be efficient, adapted to the characteristics of the region, while not affecting the environment in a bad manner, since the latter is one of the agents with the most fundamental role in energy production today (Svensson, 2010).

Among the different renewable energy sources, wind power stands out. In Brazil, wind energy has a great gen-

eration potential, besides being perennial and complementary to hydropower, which is currently the predominant power matrix in the country. Regarding the onshore wind market, the Global Wind Energy Council (2022) indicated Brazil as the country with the third largest installed capacity in the world. According to the Brazilian Association of Wind Energy and New Technologies (ABEEólica, 2022), almost 90% of this generation was represented by the Northeastern region in the year 2021. However, despite the expansion of its generation capacity in recent years with

the implementation of new wind farms, it is still difficult in Brazil to form partnerships with companies in the sector, which significantly contributes to a gap in the information available in national literature and the lack of knowledge about the mechanical behavior of wind turbines.

Thus, the Brazilian electric power company Eletrobras Furnas aims to facilitate the construction of smaller wind turbines to supply energy to more remote regions of Brazil that do not have a high generation potential through a Research and Development Project to optimize and improve modeling in

wind systems. The main objective is to evaluate the performance of this kind of structure to enable the implementation of wind farms in locations far from the Brazilian coast where there is an incidence of low-speed winds. Two relevant aspects directly linked to the performance of wind turbines are: (i) determining their natural frequency and (ii) ensuring that this frequency

## 2. Material and methods

The EOL-10 prototype was implemented in the Experimental Site I of the Furnas Civil Engineering Technology Center in Aparecida de Goiânia (GO) and is part of a project that aims for the optimization and improvement of modeling in wind power systems with appropriate experimental surveys. Therefore, to enable its implementation, a geological-geotechnical characterization of the soil was first carried out with field and laboratory investiga-

does not coincide with any external vibration frequency that the structure may experience in its life. Bouzid *et al.* (2018) stated that the accurate estimation of the natural frequency is crucial for evaluating the fatigue failure of a wind turbine structure, since it enables designers to assess the strains generated by loading cycles and determine the working life of the system.

tions. This characterization included Standard Penetration Tests (SPT), inspection shafts for *in loco* observation of the layers and soil sampling for an extensive laboratory testing campaign. More details about the whole testing campaign and its results can be found in Ferreira *et al.* (2019).

EOL-10 (Figure 1a) was assembled after site characterization. Its main components are the nacelle, the rotor, the blades, the tower, its support plates, and

Therefore, through numerical modeling using the Finite Element Method (FEM), the present article aims to list some of the main factors that can affect the prediction of the natural frequency of a real-scale wind turbine prototype and evaluate its dynamic behavior considering its rotor revolution frequency, its blade passing frequency and the wind characteristics of its operating area.

its foundation, which is a single pile piled raft. The steel tower is a tubular type with an outer diameter of 115 mm, thickness of 2.5 mm and height of 10 m. As can be seen in Figure 1b, the foundation is composed of an irregular hexagonal-shaped raft of 25 cm height with a 30 cm diameter circular pile embedded in its center and 3 m length. The piled raft reinforcement is CA-50 steel and its details are described in Alva *et al.* (2019).

## 3. Results and discussion

Prior to the natural frequency prediction of EOL-10, a calibration was performed in order to properly define the geometry, dimensions, finite element type and mesh density of the numerical model. All numerical models were implemented in Abaqus, whose mode shapes and their

respective natural frequencies are determined from eigenvalues and eigenvectors obtained through a representation of the structure by FEM. The calibration for wind turbine under free vibration was performed considering the first natural frequency, since, according to DNV-GL (2016), the

knowledge of the first natural frequency of the system can be fundamental to avoid resonance. The results showed that ground dimensions, type of finite element and mesh density of the analyzed numerical models had no relevant influence on the prediction of the wind turbine natural frequency.

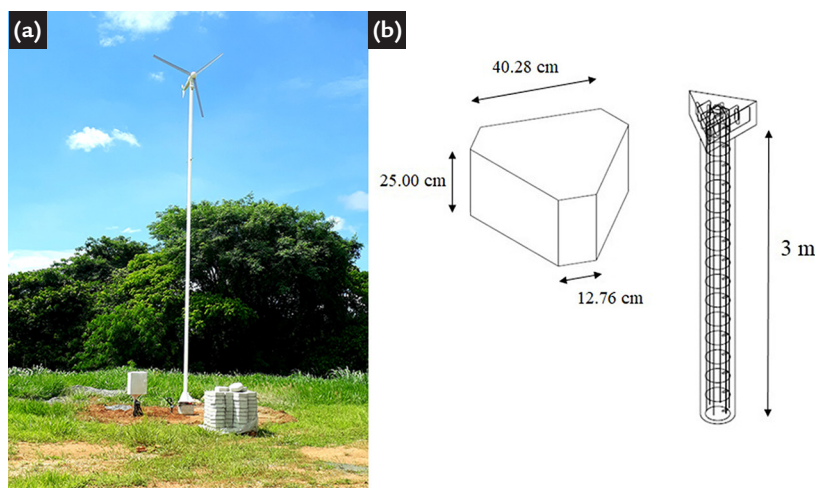


Figure 1 – EOL-10 prototype. (a) Wind turbine (Alva *et al.*, 2019); (b) Foundation.

A sensitivity analysis of a wind turbine natural frequency was also performed considering some of the main simplifications made during design that can interfere in its prediction, such as the way of considering the foundation, the soil, and the presence of the nacelle at the top of the tower. The first sensitivity analysis (Figure 2a) assumed four scenarios: (i) the

tower embedded in its base; (ii) the tower and the embedded piled raft without any surrounding material; (iii) the tower, piled raft and surrounding soil; and finally (iv) the tower and piled raft embedded in rock with unit weight and Young's modulus equal to 24 kN/m<sup>3</sup> and 20 GPa, respectively. The following sensitivity analysis (Figure 2b) was performed by comparing

the results of models with and without the nacelle. Therefore, three different models were used: (i) a full model considering the nacelle, the hub mass and three blades; (ii) a lumped mass model which replaced the nacelle, the rotor and the blades by a 100 kg point mass (sum of the mass of the system) at the top of the tower and (iii) a model without any mass at the top of the tower.

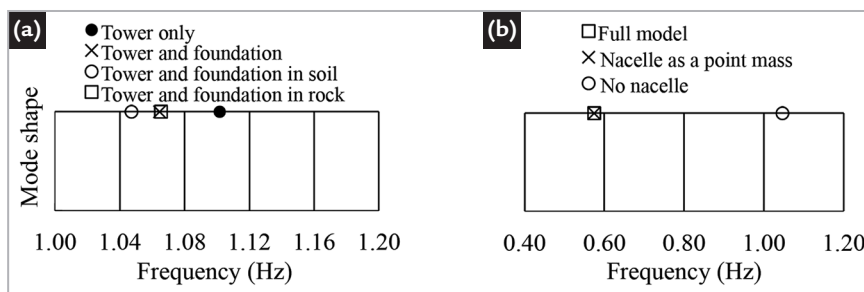


Figure 2 – Natural frequency sensitivity analysis. (a) Soil and foundation, (b) Nacelle.

One can observe that the presence of the nacelle has a great influence on the natural frequency of the wind turbine. Despite using nacelle as a lumped mass may not capture natural mode shapes that can only be observed in the full model (Huang, 2022), this simplification did not interfere in the predictions of natural frequencies, since the absolute value of its mass was the same. Therefore, according to Huang (2022), lumped mass models are frequently used in communities when it comes to designing the wind turbine towers because computation time can be greatly saved compared to that by use of the full model.

On the other hand, although using higher values of unit weight and Young's modulus for the wind turbine embedded in rock, the predictions showed only small differences in the natural frequency obtained for the model that used soil properties. This difference was not significant, probably because of the inverse effects between mass and stiffness on the natural frequency, i.e., an increment in the former tends to reduce it while an increment in the latter tends to increase it. These conflicting effects were also observed by Futai *et al.* (2018) in centrifuge tests. Furthermore, the models with embedded piled raft and piled raft embedded in rock provided very close results. This can be attributed to the threshold beyond in which there is

no additional influence of the surrounding material properties on the wind turbine natural frequency and the foundation can be assumed to be fixed. Similar results were reported by Ferreira & Futai (2016) for shallow foundations.

Based on previous results, EOL-10 was modeled with the steel tower, surrounding soil, concrete piled raft and its steel reinforcement (Figure 3), whose dimensions followed their design details. The tower was modelled by continuum shell elements, such as the piled raft and surrounding soil, whereas the concrete foundation steel reinforcement was modelled by truss elements. A 40 kg point mass equivalent to the nacelle was placed at the top of the tower.

Usually for predominantly vertical structures, such as wind turbines, the mode shapes are evaluated in the wind load direction. Therefore, the first three bending modes of EOL-10 and their respective frequencies, named  $f_{0,1}$ ,  $f_{0,2}$  e  $f_{0,3}$  were chosen for investigation. Thus, two approaches were used: (i) employing the geotechnical parameter's unit weight ( $\gamma_{nat}$ ) and Young's modulus (E), obtained by laboratory tests on undeformed samples and (ii) adopting correlations between these parameters and SPT, such as Godoy (1972) for  $\gamma_{na}$  and Ohsaki & Iwasaki (1973) for very small-strain Young's modulus  $E_0$ . A cylinder with diameter and length

equal to 6 m representing the subsoil was employed for both models. Table 1 presents the most relevant information regarding the mesh adopted for these numerical analyses.

The formulation proposed by Ohsaki & Iwasaki (1973) is quite similar to the one recommended by Petrobras (2011) for machine foundation designs and calculates the maximum small-strain shear modulus ( $G_0$ ) as a function of the SPT blow count value ( $N_{SPT}$ ) without any soil type restriction. Thus, assuming the soil as isotropic, the  $E_0$  can be obtained by its relationship with the  $G_0$  and the Poisson's ratio ( $\nu$ ), considering the value of the latter as 0.3 for all soil layers. The geotechnical properties of each numerical model obtained from SPT and the laboratory testing campaign are summarized in Table 2. The natural frequencies (NF) and their corresponding mode shapes (MS) are illustrated in Figure 4 for the two approaches used. It was observed that EOL-10 first natural frequency was not sensitive to the variation of E whose difference was approximately one order of magnitude between the two approaches. Similar results were obtained by Shi *et al.* (2023) who varied soil shear modulus from 10 to 160 MPa and observed that the wind turbine frequency  $f_{0,1}$  only slightly increases with the increasing soil shear modulus.

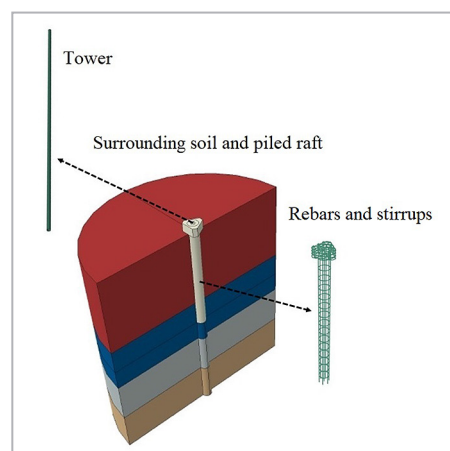


Figure 3 – EOL-10 numerical model parts.

Table 1 – General mesh details of numerical models.

Part	Element type	Number of elements
Soil	Eight-node brick element (C3D8)	13290
Tower	C3D8 with reduced integration (C3D8R)	10387
Piled raft	C3D8 with reduced integration (C3D8R)	9002
Rebars and stirrups	Two-node linear displacement (T3D2)	860

Table 2 – Geotechnical parameters of numerical models.

SPT					Laboratory				
Layer	Depth (m)	$\gamma_{nat}$ (kN/m <sup>3</sup> )	$E_0$ (MPa)	$\nu$	Layer	Depth (m)	$\gamma_{nat}$ (kN/m <sup>3</sup> )	* $E_{secant}$ (MPa)	$\nu$
1	0.0-1.0	18.00	142	0.3	1	0.0-2.3	17.70	12	0.3
2	1.0-2.0	18.00	158	0.3					
3	2.0-3.0	19.00	189	0.3					
4	3.0-4.0	19.00	173	0.3	2	2.3-3.6	17.90	18	0.3
5	4.0-5.0	18.00	142	0.3					
6	5.0-6.0	19.00	204	0.3	3	3.6-4.8	17.70	16	0.3
					4	4.8-6.0	18.10	18	0.3

\*Secant Young's modulus at 50% strength obtained from consolidated undrained triaxial tests (triaxial CU).

Methodology	$f_{0,1}$ (Hz)	1st MS	$f_{0,2}$ (Hz)	2nd MS	$f_{0,3}$ (Hz)	3rd MS
$E_{secant}^{triaxial\ CU}$	0.62		5.37		16.38	
$G_0^{SPT}$	0.62		5.41		16.61	

Figure 4 – EOL-10 natural frequencies and mode shapes.

As a comparison with the numerical models, a modal analysis was performed to determine the EOL-10 first natural frequency using an analytical formulation for a tubular profile tower with inside and outside diameters ( $\varphi$ ) according to Equations 1, 2 and 3. Thus, a simplification of the prototype (Figure 5) was adopted,

$$I = \frac{\pi}{64} \cdot (\varphi_{outside}^4 - \varphi_{inside}^4) \quad (1)$$

i.e., a 10 m length ( $L$ ) weightless beam fixed to its base with a bending stiffness ( $k_{eq}$ ) equivalent to that of the EOL-10 steel tower of, approximately, 881 N/m and with a mass ( $M$ ) of 40 kg concentrated at its top. The solution revealed a natural frequency equal to 0.75 Hz, which was very close to the prediction of a numeri-

$$k_{eq} = \frac{3 \cdot E \cdot I}{L^3} \quad (2)$$

cal model of the tower embedded in its base with zero density ( $d \approx 0$ ) and a 40 kg fixed mass at its top, but 21% higher than EOL-10 first natural frequency (0.62 Hz). This difference corroborates the warning of DNV & Risø (2002) about the error in the natural frequency prediction when assuming a completely fixed tower.

$$f_{0,1} = \frac{1}{2\pi} \cdot \sqrt{\frac{k_{eq}}{M}} \quad (3)$$

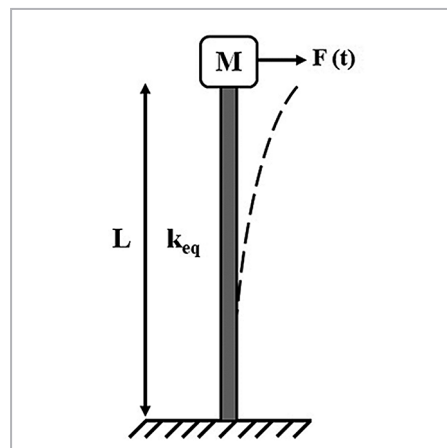


Figure 5 – Simplified model of the EOL-10.

Finally, to examine the resonance of EOL-10, the first natural frequency associated with its first bending mode ( $f_{0,1}$ ) was compared with its rotor revolution frequency ( $f_{1p}$ ) and the blade passing frequency ( $f_{3p}$ ). According to the manufacturer's information and the prototype's monitoring data set, the EOL-10 rotor frequency is in the range of 0.3 to 2 Hz. Thus,  $f_{3p}$ , which is the frequency of the aerodynamic pulses induced by the passage of each blade, should vary between 0.9 and 6 Hz. Figure 6 indicates that  $f_{0,1}$  of EOL-10 is within the range of  $f_{1p}$  and  $f_{3p}$ .

It can be observed that the EOL-10 first natural frequency is not within the safety margin indicated in the DNV-GL (2016) guidelines. However, this requirement may be omitted if countermeasures are in place to prevent resonance effects, in particular an operational vibration monitoring system or damping devices

(DNV-GL, 2016). EOL-10 is instrumented with sensors distributed along its tower height that provide real-time acceleration, tilt, and force measurements to monitor its structural integrity.

It is also necessary to verify that the natural frequency of the system does not coincide with any external vibration force that the structure may experience during its service life and can cause large displacements. As an example, a steady-state dynamic analysis was performed in Abaqus, which calculates EOL-10 response based on its natural frequencies and mode shapes. Such analysis is done as a frequency sweep by applying the loading at a series of different frequencies. Thus, there was considered a set of forces composed of (i) a horizontal load concentrated at its top equal to 60 N and (ii) a triangular distributed load on half of the tower lateral area varying

from zero at its base to approximately 55 N/m<sup>2</sup> at its top. Figure 7 shows the displacements at the top of the EOL-10 tower, if the prototype is subjected to forces with application frequencies close to its  $f_{0,1}$ . These forces were computed considering the wind characteristics obtained from the meteorological data system of the Furnas experimental site. Thereby, they were calculated considering the highest wind speeds recorded so far, i.e., 3.6 m/s. Assuming a structural damping of 5% for the whole system, the predictions showed that if wind loads act on the tower with a frequency close to 0.6 Hz, the displacement at the top of the tower can reach almost 1 m. It is worth mentioning that, since y-axis represents the magnitude of displacements, the sudden drop to zero displacement around 0.6 Hz in Figure 7 was caused by a change of displacement sign.

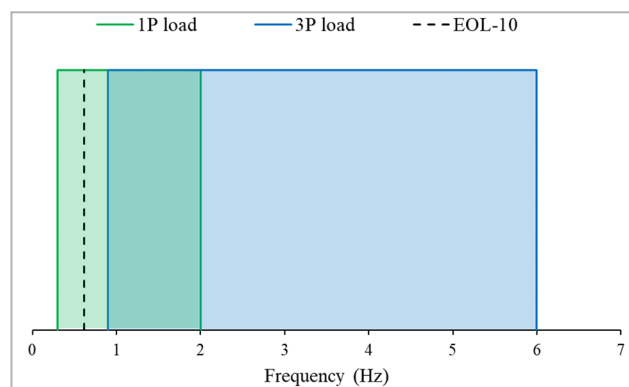


Figure 6 – Resonance check for EOL-10.

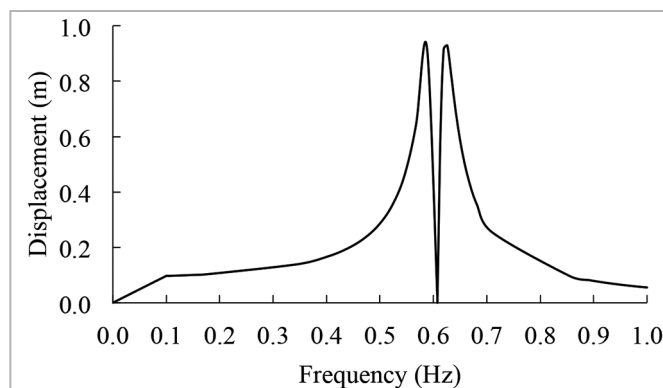


Figure 7 – Tower top displacements after wind loads at different application frequencies.

## 4. Conclusions

Through numerical modeling, the present research studied the dynamic behavior of a wind turbine prototype located in the Midwestern Region of Brazil, considering its rotor revolution frequency, its blade passing frequency and the wind characteristics of its operating area, together with investigating some of

the main factors that may interfere with the prediction of its natural frequency. When studying the natural vibration frequencies, it was evidenced that the consideration of the nacelle interfered substantially in the natural frequency of the tower, and that the influence of the surrounding soil properties on the frequency

of the whole system was not very expressive, probably because of the inverse effects between mass and stiffness on the natural frequency, i.e., an increment in the former tends to reduce it, while an increment in the latter tends to increase it. Soils with higher unit weights are usually stiffer. Furthermore, it is assumed that

the completely fixed tower may induce a relevant difference during the prediction of a wind turbine first natural frequency.

To examine the resonance according to DNV-GL (2016), although the first natural frequency of the EOL-10 is within the range of the excitation frequencies of its rotor and the passing fre-

quencies of its blades, it is instrumented with sensors to monitor its structural integrity in real time. A dynamic analysis of the wind effects showed that, if the loads act on the tower with a frequency close to its natural frequency, the displacements at its top can be significant. Finally, although clarifying some aspects

about geotechnical design of wind turbines, the conclusions presented in this article are still limited to EOL-10 and its operating area. Further analyses should be carried out for different wind turbine configurations, foundations and sites with the main purpose of corroborating the results obtained.

## Acknowledgments

The authors would like to thank the Brazilian National Council for Scientific and Technological Development (CNPq), the Brasília Research Foundation (Finatec), the Foundation and Field Test Group (GPFees) of the University

of Brasília Geotechnical Post Graduate Program and the Brazilian electric power company Eletrobras Furnas for logistical and financial support. This research was based upon a R&D Project from AN-EEL - National Agency, "Otimização do

modelo meteorológico BRAMS, com validação experimental, para subsidiar aperfeiçoamentos de modelagens em sistemas eólicos" – PD-0394-1709/2017, supported by Eletrobras Furnas with University of Brasília cooperation.

## References

- ALVA, F. J. G.; MATOS, Y. M. P.; FARIAS, M. M.; CUNHA, R. P.; GUIMARÃES, M. J. R. Análise dinâmica de um gerador eólico em solo tropical. *In: SIMPÓSIO DE PRÁTICA DE ENGENHARIA GEOTÉCNICA NA REGIÃO CENTRO-OESTE – GEOCENTRO, 5.*, Brasília, 2019. *Anais [...]*. Brasília: ABMS, 2019. p. 118-127.
- ASSOCIAÇÃO BRASILEIRA DE ENERGIA EÓLICA E NOVAS TECNOLOGIAS. *Annual wind energy report 2021*. 2022. Available in: [https://abeolica.org.br/wp-content/uploads/2022/01/Relatorio\\_ABEEÓLICA\\_2022.pdf](https://abeolica.org.br/wp-content/uploads/2022/01/Relatorio_ABEEÓLICA_2022.pdf). Accessed in: 10 abr. 2023.
- BOUZID, D. A.; BHATTACHARYA, S.; OTSMANE, L. Assessment of natural frequency of installed offshore wind turbines using nonlinear finite element model considering soil-monopile interaction. *Journal of Rock Mechanics and Geotechnical Engineering*, v. 10, p. 333-346, 2018. DOI: 10.1016/j.jrmge.2017.08.006.
- DNV - RISØ. *Guidelines for design of wind turbines*. 2002. Available in: [https://www.windpower.org/media/1031/design\\_of\\_wind\\_turbines\\_2002.pdf](https://www.windpower.org/media/1031/design_of_wind_turbines_2002.pdf). Accessed in: 12 abr. 2023.
- DNV-GL. *Standard DNV-GL-ST-0126: Support structures for wind turbines*. 2016. Available in: <https://rules.dnvgl.com/docs/pdf/DNV/codes/docs/2016-01/DNVGL-ST-0126.pdf>. Access at: 12 abr. 2023.
- FERREIRA, Y. A.; FUTAI, M. M. Análise do comportamento das fundações de torres eólicas. *In: COBRAMSEG, 18.*, Belo Horizonte, 2016. *Anais [...]*. Belo Horizonte: ABMS, 2016. 8 p.
- FERREIRA, J. R.; SCHLIEWE, M. S.; CABRAL, R. M.; CÔRTEZ, H. A. Caracterização do Campo Experimental I do Centro Tecnológico em Engenharia Civil de Furnas. *In: SIMPÓSIO DE PRÁTICA DE ENGENHARIA GEOTÉCNICA NA REGIÃO CENTRO - OESTE – GEOCENTRO, 5.*, Brasília, 2019. *Anais [...]*. Brasília: ABMS, 2019. p. 161-164.
- FUTAI, M. M.; DONG, J.; HAIGH, S. K.; MADABHUSHI, S. P. G. Dynamic response of monopiles in sand using centrifuge modelling. *Soil Dynamics and Earthquake Engineering*, v. 115, p. 90-103, 2018. DOI: 10.1016/j.soildyn.2018.08.026.
- GLOBAL WIND ENERGY COUNCIL. *Global wind report 2022*. 2022. Available in: [https://gwec.net/wp-content/uploads/2022/03/GWEC\\_Global\\_Wind\\_Report\\_2022\\_Web.pdf](https://gwec.net/wp-content/uploads/2022/03/GWEC_Global_Wind_Report_2022_Web.pdf). Accessed in: 10 abr. 2023.
- GODOY, N. S. *Fundações*. São Paulo: Escola Politécnica da Universidade de São Paulo, 1972. (Notas de aula).
- HUANG, H. S. Dynamic analysis of 10 mega-watts offshore wind turbine under wind and coupled wind-ocean-wave loads. *Composite Structures*, v. 291, n. 115497, 2022.
- OHSAKI, Y.; IWASAKI, R. On dynamic shear moduli and Poisson's ratio of soil deposits. *Soils and Foundations*, v. 13, n. 4, p. 59-73, 1973.
- PETROBRAS. *N-1848: projeto de fundações de máquinas*. Rio de Janeiro: Petrobras, 2011.
- SHI, Y.; YAO, W.; JIANG, M. Dynamic analysis on monopile supported offshore wind turbine under wave and wind load. *Structures*, v. 47, p. 520-529, 2023.
- SVENSSON, H. *Design of foundations for wind turbines*. Dissertation. Lund University, Lund, 2010.

Received: 19 April 2023 - Accepted: 28 July 2023.



All content of the journal, except where identified, is licensed under a Creative Commons attribution-type BY.